

Comparative evaluation of drying techniques for surface micromachining

Chang-Jin Kim ^{*}, John Y. Kim ¹, Balaji Sridharan

Mechanical and Aerospace Engineering Department, University of California, Los Angeles, CA 90095-1597, USA

Abstract

Five different procedures commonly used to rinse and dry released microstructures are compared: evaporation drying with deionized (DI) water or methanol, sublimation drying with *t*-butyl alcohol or *p*-dichlorobenzene, and supercritical drying with CO₂. For objective comparison, identical test structures, made by the MCNC Multi-User MEMS Processes (MUMPs), are used in evaluating the drying techniques. The test chips contain arrays of surface-micromachined polysilicon cantilevers (2 μm thick, 2 μm gap from the substrate) with varying widths and lengths. Some beams feature dimples or tips to quantify their anti-stiction effect. This study reveals, for the first time, that the maximum beam length obtainable increases as the beam width increases for the cases of sublimation and supercritical drying, opposite to the previously known case of evaporation drying. Both sublimation drying methods as well as supercritical drying rendered good results, releasing cantilevers up to 700 μm in length without stiction. We also introduce a new setup that considerably improves the way sublimation is used to dry microstructures. © 1998 Elsevier Science S.A.

Keywords: Release methods; Stiction; Surface micromachining

1. Introduction

The relative importance of the surface effect, compared with other physical effects, grows as mechanical elements shrink in size. Normally a negligible factor for mechanical devices in the conventional (macro) world, the surface effect emerges as a relevant issue as objects become smaller than millimeters [1], as nature indicates [2]. Faced by the unprecedented task of dealing with mechanical devices orders of magnitudes smaller than previously known, designers have to understand the role of surface forces in manufacturing micromechanical devices as well as in their performance.

Adhesion of microstructures to neighboring surfaces, typically the substrate, is one of the main difficulties in surface micromachining due to the inherent proximity (less than a few microns) between the freed structures and the underlying substrate. This phenomenon is more commonly called 'stiction' in the field of microelectromechanical systems (MEMS). Stiction includes the more complex situation of two surfaces rubbing each other.

The most generic procedure to obtain free-standing surface-micromachined structures is to rinse the etchant used to free the structures with deionized (DI) water and simply dry

it through evaporation. A flexible microstructure is pulled down to the substrate during drying by the capillary pressure induced by the droplet in the gap. If the adhesion force between the contacted areas is larger than the elastic restoring force of the deformed structure, the structure remains stuck to the substrate even after being completely dried. Studies have shown that solid bridging, van der Waals force, electrostatic forces, and hydrogen bonding are among those responsible for this stiction phenomenon [3,4]. A theoretical analysis has provided a mathematical relation between the longest cantilever free of stiction, or detachment length, and beam dimension, Young's modulus, and surface energy [5,6].

There are two different general directions to address the adhesion problem of flexible micromechanical elements. One strategy is to prevent the structures from coming into direct contact with the substrate during the drying step. Several techniques have been developed over the years to solve this so-called 'process-related', 'fabrication-related', or 'release-related' stiction, and more description follows soon. However, even after the elements are freed and dried successfully, they may come in brief contact with the substrate during packaging, transportation, or by various reasons such as dropping, thermal distortion, charge accumulation, or over-range driving during operation. In this case, capillary condensation [7,8] is likely to occur in the gap, turning the situation back to the generic evaporation drying step. The

^{*} Corresponding author. Tel.: +1 310 825 02 67. Fax: +1 310 206 23 02. E-mail: cjkim@seas.ucla.edu

¹ Present address: Allied Signal Inc., Aerospace Equipment Systems, MS 36-1, 2525 W. 190th St, Torrance, CA 90504, USA.

other strategy is to prevent this so-called ‘in-use’ stiction by modifying the contacting surface. The surface is modified to a hydrophobic or to a lower surface-energy state so that the capillary condensation is prevented or adhesion force is reduced, either chemically (truly) [9–11] or physically (effectively) [12,13].

This paper studies the techniques used to alleviate the fabrication-related stiction and provides an objective comparison of five different methods commonly used in drying released microstructures. Evaporation of DI water is considered as a basic, reference procedure. One simple method to reduce the capillary pull-down force is to use a low surface-tension liquid such as methanol as the final rinse. A more effective way is to eliminate the capillary effect altogether by avoiding formation of the liquid–gas interface in the first place. This goal can be reached by solidifying the final rinsing liquid followed by sublimating [14–16] or ashing it [17], or pressurizing and heating it above supercritical point and venting under constant temperature [18]. Fig. 1 shows the trajectory of the pressure–temperature state the final rinse follows during the drying process for evaporation, sublimation, and supercritical drying. A different approach is to build temporary polymer structures, reinforcing flexible microstructures during drying, and removing the polymer in plasma as the final step. This procedure can be employed with [19] or without [20] modification of the original device.

The five different drying techniques selected for comparison in this paper are: (1) evaporation drying of DI water, (2) evaporation drying with methanol, (3) sublimation drying with *t*-butyl alcohol, (4) sublimation drying with *p*-dichlorobenzene, (5) supercritical drying with CO₂. All of these procedures have been used by others before. However, each has been developed and tested with different facilities to release different microstructures, so that objective evaluation and comparison are not available. Furthermore, some of the techniques are highly dependent on the operator’s skill, rendering a comparison based on the reported results from different sources unreliable. In this paper, identical test chips with surface-micromachined polysilicon beams obtained from the same fabrication lot are used to evaluate objectively the relative effectiveness of each drying procedure tested.

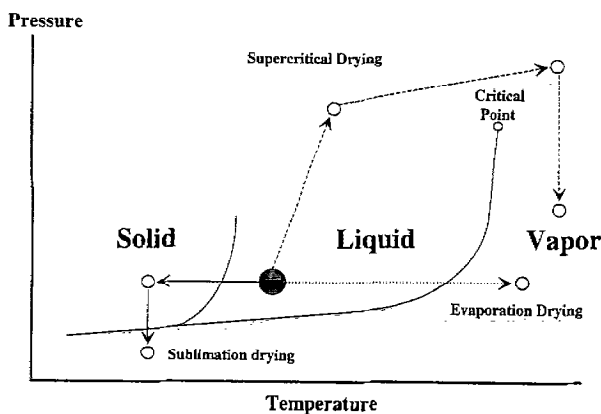


Fig. 1. *P*–*T* graph for various drying procedures.

Cantilevers with varying widths and lengths are used as test structures. Some beams feature anti-stiction dimples or tips. The detachment length is obtained for each of the tested drying procedures, and the effect of width on the detachment length is discussed based on the experimental results. The effects of dimples and anti-stiction tips are also discussed. In the course of sublimation experiments, an improved sublimation setup and technique are developed to cope with the many repeated procedures needed in this project. However, no special attempt has been made to perfect any of the tested procedures in order to keep the objectiveness.

2. Test beams

Test structures have been designed to use the MCNC Multi-User MEMS Processes (MUMPs) [21], which pro-

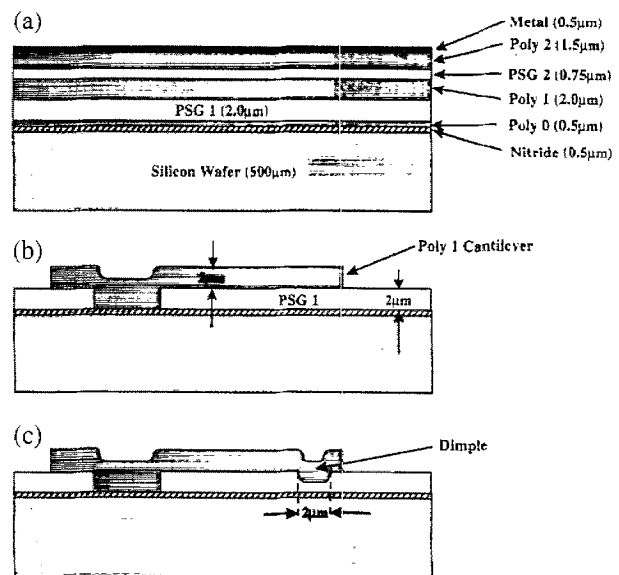


Fig. 2. Test structure fabrication: (a) deposited layers for MUMPs; (b) cross section of a Poly 1 cantilever beam (before release); (c) cross section of a Poly 1 cantilever with a dimple (before release).

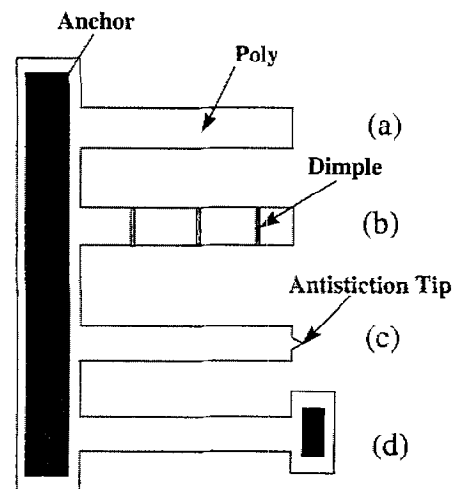


Fig. 3. Test structures: (a) cantilever; (b) cantilever with dimples; (c) cantilever with antistiction tip [22]; (d) doubly clamped beam.

vide popular features of the surface-micromachining process: (1) polysilicon as the structural layer, (2) phosphosilicate glass (PSG) as the sacrificial layer, and (3) silicon nitride as the electrical isolation layer on the substrate. Repeatability of an established fabrication process has been valued as well as the convenience of using the multi-user process, so that similar test structures can be used in the future, in case more releasing techniques are to be evaluated.

Layers deposited during the MUMPs are shown in Fig. 2(a). First, the surface of the wafer is heavily doped with phosphorus, and a 5000 Å thick LPCVD nitride layer is deposited. Three polysilicon and two PSG layers are then deposited by low-pressure chemical vapor deposition (LPCVD). Each layer (except nitride) is patterned by reactive ion etching (RIE) according to the design layout. For example, a cantilever pattern of 2 μm thick Poly 1 layer is shown in Fig. 2(b), which will be suspended over the substrate by 2 μm defined by the thickness of PSG 1. The same Poly 1 cantilever with a dimple is shown in Fig. 2(c). After

MUMPs is completed, microbeams are released and dried by one of the drying methods studied here.

Cantilevers and doubly clamped beams (bridges) using Poly 1 as structural layers were designed and tested. The test structures have varying width (2, 3...9, 10, 15, 20 μm) and length (50–1000 μm in 25 μm increments). We obtained the detachment lengths of polysilicon beams for each beam width for different release methods. The same procedure was repeated for beams with added anti-stiction features as shown in Fig. 3.

3. Experiments

Many identical MUMPs chips were used to test the five different drying procedures: DI water and methanol evaporation, *t*-butyl alcohol and *p*-dichlorobenzene sublimation, and CO₂ supercritical drying. For each sample, concentrated HF (49%) is used for etching the PSG sacrificial layer for

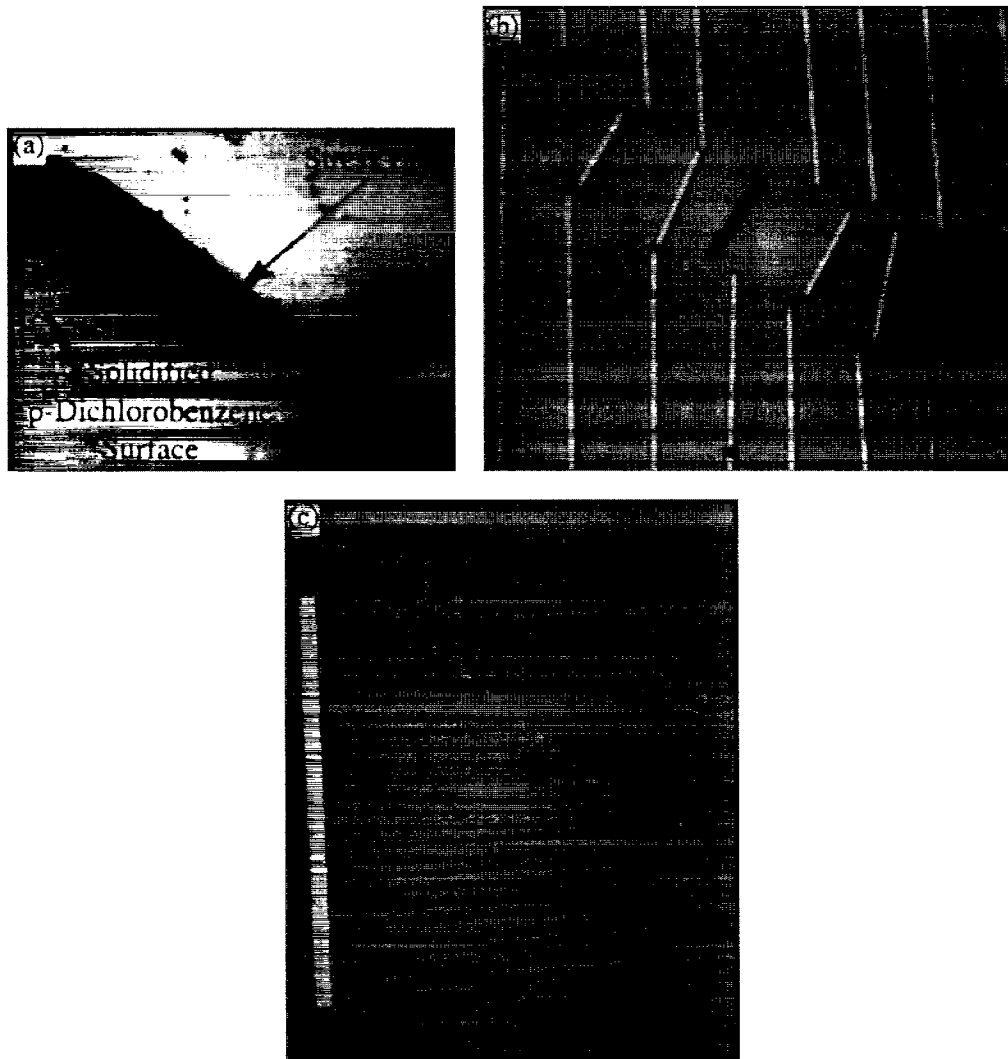


Fig. 4. Adverse effects of rapid solidification of *p*-dichlorobenzene: (a) crack in the solidified chemical; (b) beams broken by the stress crack; (c) doubly clamped beams broken at constraints.

about 2.5 min (recommended by MUMPs) before introducing the sample in DI water for neutralizing and rinsing HF.

3.1. Evaporation drying

Following the PSG etching with HF, the sample is immersed in a large volume of continuously flowing DI water for 30 min. Long rinsing in high-quality DI water helps to reduce the accumulation of residual particles under the beam and the effect of solid bridging. Careful handling of the sample is critical for all of the procedures tested in this paper due to the presence of many unusually long and flexible beams. Agitation in liquid could significantly deform or even break the longer and more flexible cantilevers, causing the deformed or broken beams to land on other structures. For methanol evaporation drying, DI water was replaced with methanol by three steps, each time immersing the chip in fresh methanol for 10 min. Samples from DI water or methanol were then placed inside a 100°C oven for approximately 20 min to ensure complete removal of the liquid from the samples.

3.2. Sublimation drying

Because of the solubility of methanol in both of the sublimation liquids tested (*t*-butyl alcohol [15] and *p*-dichlorobenzene [16,23]), DI water is replaced with methanol first. Methanol is then replaced with the sublimation liquid. The melting temperature of *t*-butyl alcohol (26°C) is near room temperature. After replacing methanol, the chemical should be solidified and sublimated inside a refrigeration system. On the other hand, *p*-dichlorobenzene has a melting temperature of 56°C. The chemical should be melted on a hot plate before replacing methanol, but solidification and sublimation are done at room temperature.

As we implemented the two sublimation methods to dry our test chips, some difficulties that negatively affect the process time and yield have been identified. We learnt that *t*-butyl alcohol absorbs water vapor from ambient air when cooled below room temperature or left open to air for an extended period. Solidifying in a refrigerator and transporting the chip into a vacuum setup would cause moisture condensation. Any amount of water introduced to our sample precipitates in the small gap during the sublimation and can drastically reduce the yield. For the case of *p*-dichlorobenzene, rapid solidification at room temperature creates high stress in the solidified chemical, as shown in Fig. 4(a). Constrained structures are damaged by this stress, while cantilevers suffer much less. The failure could apparently be caused by the cracks formed in the solidified chemical (Fig. 4(b)) or by the structure's inability to comply with overall shrinkage of the chemical (Fig. 4(c)). Structures with high compliance do not suffer from the same procedure [23]. For good results, temperature control (e.g., a programmable hot plate) is needed to slow down the cooling speed.

A new sublimation setup (Fig. 5) was needed to address the above issues. The key idea is the use of a thermoelectric (Peltier) chip which acts as either a miniature heater or refrigerator based on the electric polarity. The Peltier chip is small and simple enough to be placed inside the vacuum chamber (a bell jar) and controlled electrically from outside. For the *t*-butyl alcohol sublimation, solidifying and sublimation can be done without breaking the vacuum, which prevents moisture from being introduced to the chemical. Using the new sublimation setup, significantly improved results have been achieved. For the *p*-dichlorobenzene sublimation, a chip is placed on a heated Peltier chip, and its cooling speed can be controlled electrically to reduce stress in the solidifying chemical.

In addition to providing the above process solution, the developed tabletop setup has other advantages. It accommodates both *p*-dichlorobenzene and *t*-butyl alcohol sublimation drying and eliminates the need for a hot plate and the bulky refrigeration setup used in the past. Since the Peltier chip is placed inside the vacuum chamber (a bell jar), the setup is

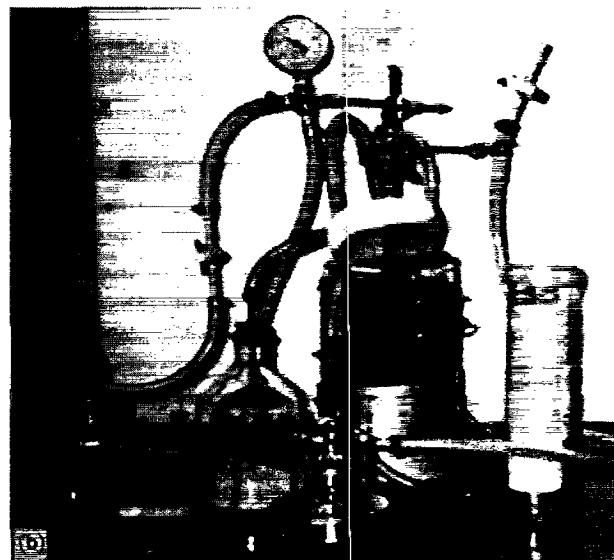
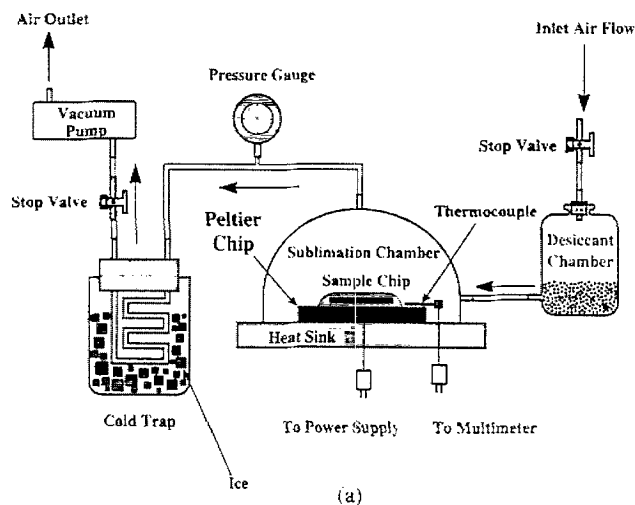


Fig. 5. Sublimation setup: (a) schematic figure; (b) photograph.

simplified and dramatically reduced in overall size. In addition to the improved process yield and lower cost of the setup, the process time was reduced due to the simple operation of the Peltier chip. Since the vapor pressure of *t*-butyl alcohol (27 torr at 20°C) is over 10 times higher than that of *p*-dichlorobenzene (1 torr at 25°C), sublimation of *t*-butyl alcohol is much quicker. For a 1 cm² chip in our current systems, sublimation takes 15 min for *t*-butyl alcohol and 3 h for *p*-dichlorobenzene.

3.3. CO₂ supercritical drying

A CO₂ supercritical drying setup in UCLA's Nanolab was used. The released sample was placed on a boat filled with methanol before placing it inside the setup. Carbon dioxide filling and methanol flushing were repeated 10 times to ensure complete removal of methanol from the chamber. The chamber pressure rises from 800 psi to 1350 psi when the temperature, initially ≈ 17°C, is brought above the supercritical temperature (≈ 40°C) of carbon dioxide (see Fig. 1). As carbon dioxide is vented out of the chamber slowly, maintaining the temperature roughly constant, the pressure is lowered back to the atmospheric pressure without condensation.

4. Results and discussion

The test results for two sets of beams are summarized in Fig. 6. Fig. 6(a) is for flat cantilever beams (see Fig. 3(a)), and Fig. 6(b) is for cantilevers with dimples every 50 μm along the beam (see Fig. 3(b)). Each data point indicates the detachment length, the longest cantilever successfully freed without stiction, for a given beam width. The detachment length is sensitive to parameters such as surface roughness and slight variation in handling, and the data are known to scatter [6]. However, finding general trends being our main goal, statistical analysis has not been attempted in this paper.

4.1. Evaporation drying

The sequence leading to stiction starts first by a liquid droplet in the gap pulling down the beam to the substrate. If the beam is stiff (i.e., short) enough, the beam would not bend much, and drying proceeds from the tip of the beam to the base as depicted in Fig. 7 [22]. Stiction would not occur in this case. On the other hand, a flexible (i.e., long) beam will bend down enough so that a droplet is formed near the tip as depicted in Fig. 8. As rinsing liquid starts to evaporate

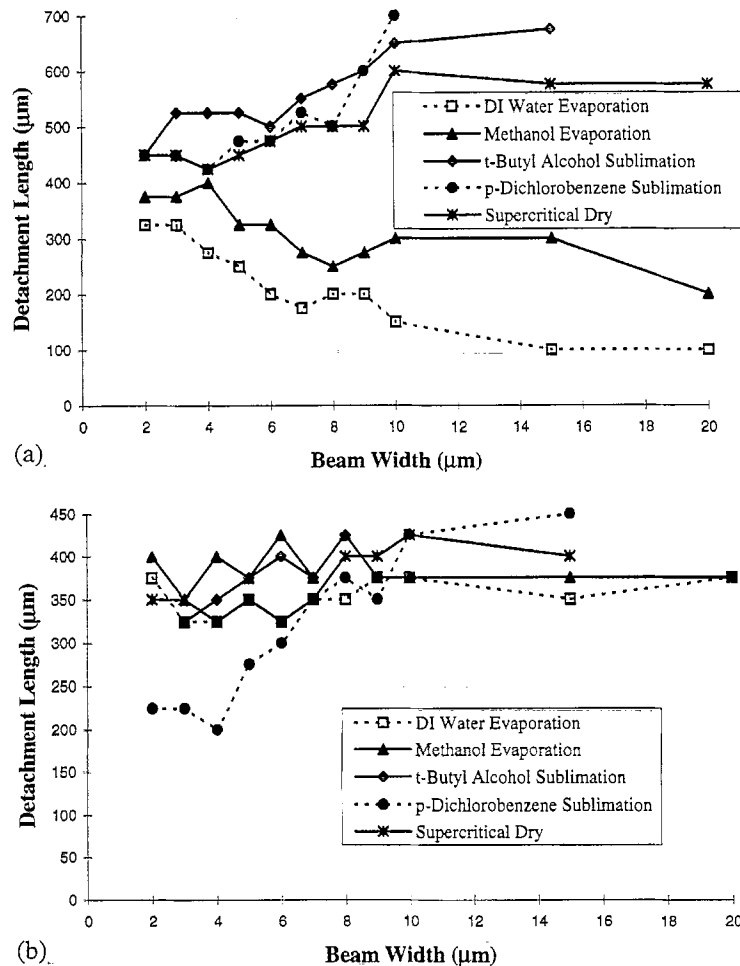


Fig. 6. Detachment length vs. beam width: (a) flat cantilevers; (b) cantilevers with dimples.

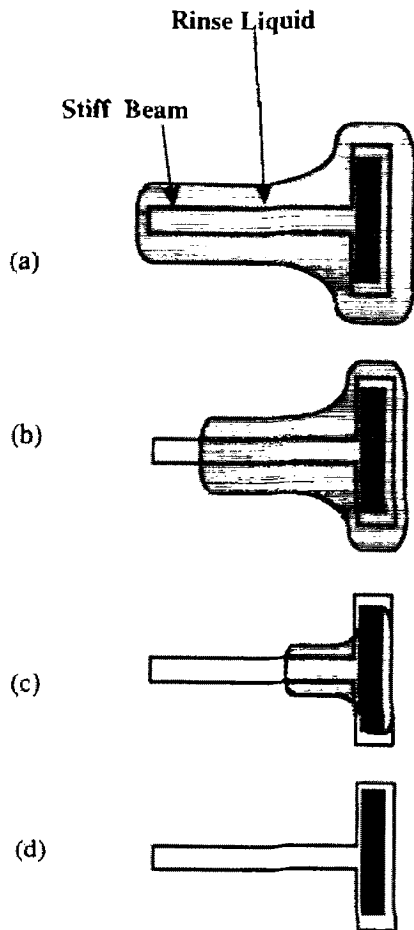


Fig. 7. Evaporation drying of short cantilever.

(Fig. 8(a) and (b)), necking of the liquid occurs near the base (Fig. 8(c)), and as time proceeds a discontinuous droplet is formed below the tip of the beam (Fig. 8(d) and (e)). As this droplet evaporates it may pull down the beam into contact with the substrate, after which it remains pinned down if the surface adhesion force is greater than the elastic restoring force of the beam.

From Fig. 6(a) we can see that methanol evaporation provides a larger detachment length than DI water evaporation, as expected due to the lower surface tension of methanol. For both of the evaporation drying methods, the detachment length decreases as the beam width increases. This length versus width relationship can be explained with Fig. 8, which compares two cantilevers of different beam widths. The detachment length increases as the beam becomes stiffer and decreases as the pull-down force increases. Since capillary pressure is the dominant component [7], the pull-down force is approximately proportional to the projected area of the droplet. Due to the tendency of the droplet to be circular (to minimize the free surface area), it is expected that the liquid area is proportional to approximately the square of the beam width. On the other hand, the restoring elastic energy stored in the beam is linearly proportional to the beam width. Hence the liquid pull-down energy increases at a greater rate than the restoring elastic energy as the beam width increases.

Assuming the contact area is proportional to the droplet area, a similar trend is expected between the surface adhesion energy and beam restoring energy. For this reason, the detachment length decreases as the beam width increases for evaporation drying.

The above argument of droplet area being proportional to the square of the beam width assumes the beam is long and flexible enough to have the tip of the pulled-down beam reasonably flat on the substrate. The assumption does not extend to shorter beams, however, which start to exhibit the effect of tip slope. For short cantilevers, the droplet area and the resulting pull-down force become more sensitive to the beam length than width. Eventually, all beams below a certain length fall into the situation shown in Fig. 7 and will be freed without stiction. From Fig. 6(a) it can be seen that the detachment length stops decreasing below a certain beam length (for example, roughly below 100 μm for DI water evaporation) regardless of width.

The existence of dimples affects the result of the evaporation drying greatly, as shown in Fig. 6(b). In addition to the improvement over the flat beams, it is clearly seen that the detachment length is not sensitive to the beam width when dimples are used. The dimples in this paper are 2 μm along the beam length direction but made over full width (see Fig. 2(c) and 3(b)). As the drying of rinse liquid proceeds, the droplet is expected to form under the dimple where the gap is smallest. Since the length of the dimple is constant (2 μm), the droplet area and the resulting capillary pull-down force may be constant or proportional to the width at best. This is in contrast to the case of flat beams, where the pull-down force is proportional to the width squared. Most importantly, the surface adhesion energy is proportional to the dimple area, which is proportional to the beam width:

$$E_{\text{ad}} = \gamma_s A_c = (\gamma_s l) w$$

where γ_s is the interfacial adhesion energy per unit area, A_c is the contact area, E_{ad} is the adhesion energy between the two contacting surfaces, l is the length of the dimple (2 μm), and w is the beam width. Since the restoring elastic energy of the beam is also proportional to the width, the detachment length stays approximately constant as beam width varies.

A triangular shaped antistiction tip shown in Fig. 3(c), 5 μm base and 6 μm long, was added to a set of beams with 10 μm width and varying lengths. For both evaporation drying methods, the detachment length was nearly identical to that of the 10 μm beam with dimples. The agreement of the two results can be explained by the fact that the droplet area and resulting contact adhesion area are approximately equal for these two cases (5 $\mu\text{m} \times 6 \mu\text{m} \times 0.5 \cong 15 \mu\text{m}^2$ for the antistiction tip and 10 $\mu\text{m} \times 2 \mu\text{m} = 20 \mu\text{m}^2$ for the dimple).

4.2. Sublimation and supercritical drying

All three drying techniques that avoid formation of a liquid-gas interface, i.e., *t*-butyl alcohol sublimation, *p*-dichlorobenzene sublimation, and CO_2 supercritical release,

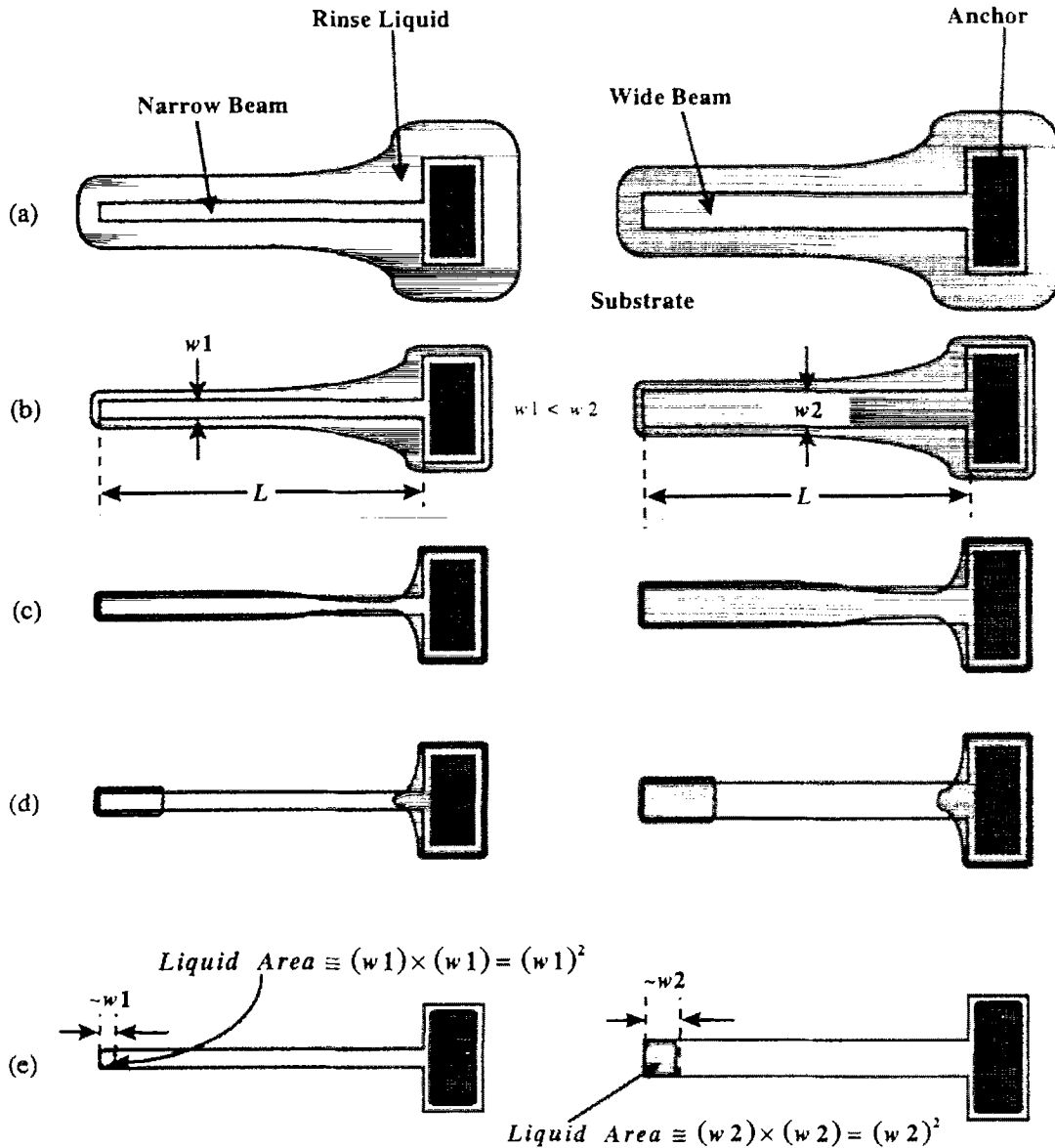


Fig. 8. Evaporation drying of long cantilever with two different beam widths.

performed better than evaporation drying for flat cantilevers, as Fig. 6(a) indicates. An interesting trend has been found for the relationship between the detachment length and beam width. As the beam width increases, the detachment length

also increases. This trend is opposite to that of evaporation drying. A speculation is given below to explain the trend.

To understand the pull-down force created during sublimation, a possible drying sequence is shown in Fig. 9. As the

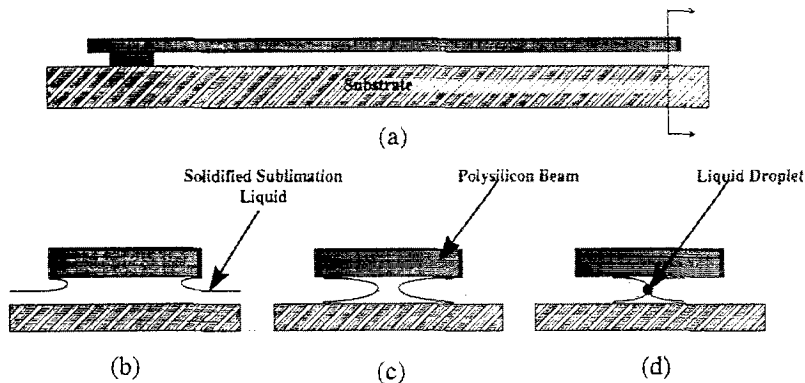


Fig. 9. Possible sequence of sublimation drying: (a) side view; (b) initial stage; (c) necking; (d) droplet condensation.

solidified chemical sublimates off from underneath the beam, necking occurs and a solid bridge forms (Fig. 9(c)). When this bridge is eventually broken, a small amount of trace moisture may condense at the broken tips and thus reattaches the bridge (Fig. 9(d)). This sequence may ultimately cause the beam to come in contact with the substrate if the beam is flexible enough. In this scenario, the area of the moisture droplet is nearly identical regardless of the beam width. Since elastic energy in the beam is proportional to the width, wider beams would result in a longer detachment length.

For CO₂ supercritical drying, a trace of methanol or water moisture remaining in the system is suspected to contribute to stiction. Since only a minute amount of moisture is present in the vacuum system, the amount of condensation underneath the beams is expected to be limited regardless of the beam width or shape.

Dimples and antistiction tips do not play a distinctive role for the cases of sublimation and supercritical drying. The advantage of sublimation and supercritical drying over evaporation drying is not apparent when anti-stiction dimples are used, as Fig. 6(b) indicates. However, it should be noted that sublimation and supercritical drying techniques can be improved much further, such as reducing the moisture content in the system, while evaporation techniques do not have as much potential for future improvement.

5. Summary and conclusions

This work has compared, using identical test chips, various drying techniques commonly employed for polysilicon surface micromachining. The results are summarized in Table 1. Two newer techniques, HF vapor-phase etching (VPE) [24,25] and use of a self-assembled monolayer (SAM) antistiction coating [11], have not been tested for the current test devices. The test devices used for this work were fabricated differently from those used for SAM [11] and HF vapor phase release [24,25] in that the test devices did not have a polysilicon ground plane. The SAM coating was however tested on other devices and proved to be effective in decreasing stiction.

Problems with existing sublimation procedures have been identified, and an improved setup has been developed for sublimation drying. The new tabletop setup provided us with consistent results fast and conveniently. *T*-butyl alcohol sublimation proved to be fast, clean, and effective with our setup, which allows a good control of sample temperature while keeping it under vacuum. *p*-dichlorobenzene sublimation could be equally effective, although the chemical is rather toxic and sublimation takes longer due to its lower vapor pressure. Among the methods tested, CO₂ supercritical drying proved to be the most consistent and clean method. It was found that an increase in beam width has a positive effect on detachment length for sublimation and supercritical drying and a negative effect for evaporation drying. Explanations of the two different trends are provided.

Table 1
Summary of release methods

Release methods	Evaporation drying		Sublimation drying		Supercritical drying		HF VPE ^a	SAM coating ^a
	HF → DI water	HF → DI water → methanol	HF → DI water → methanol → <i>t</i> -butyl alcohol	HF → DI water → methanol → <i>p</i> -dichlorobenzene	HF → DI water → methanol → carbon dioxide	HF vapor		
Melting temp. (°C)	0	~97.5	26	56	~56.4	~83.2	N/A	HF → DI → H ₂ O → DI → IPA → CCl ₄ OTS → IPA → DI
Boiling temp. (°C)	100	64.7	82.2	173	~78.3	20	N/A	
Vapor pressure (torr)	17.54 @20°C 355.3 @80°C	140 @27°C	27 @20°C	1.03 @25°C 10 @54.8°C	N/A	687.8 @17°C	N/A	
Surface tension (mN m ⁻¹)	72.88 @25	22.65	20.17	N/A	1.16	N/A	N/A	
Advantages	simple	lower surface tension than DI water	fast sublimation	only hot plate needed	clean excellent results	no liquid involved excellent results	no complicated setup excellent results	many chemicals and rinsing steps
Disadvantages	mediocre results	mediocre results	requires refrigeration and vacuum absorbs water vapor	toxic needs vacuum contracts upon solidifying	complicated setup	complicated setup under development		

^a Not tested for this paper.

Acknowledgements

This project has been partially supported by the Defense Advanced Research Projects Agency (DARPA) under DABT63-95-C-0050. The authors would like to thank the entire UCLA Micromanufacturing Laboratory staff for their support and assistance.

References

- [1] Class note, Microelectromechanical Systems (MEMS): Mech and AE 280, University of California, Los Angeles (UCLA). See also Micro Electro Mechanical Systems (MEMS), a short course offered by UCLA Extension, 10995 Le Conte Avenue, Los Angeles, CA 90024.
- [2] T.A. McMahon and J.T. Bonner, *On Size and Life*, Scientific American Books, New York, 1983, p. 221.
- [3] R.L. Alley, G.J. Cuan, R.T. Howe and K. Komvopoulos, The effect of release-etch processing on surface microstructure stiction, Solid-State Sensors and Actuator Workshop, Hilton Head Island, SC, USA, 1992, pp. 202–207.
- [4] R. Legtenberg, H.A.C. Tilmans, J. Elders and M. Elwenspoek, Stiction of surface micromachined structures after rinsing and drying: model and investigation of adhesion mechanisms, *Sensors and Actuators A*, 41–43 (1994) 230–238.
- [5] C.H. Mastrangelo and C.H. Hsu, Mechanical stability and adhesion of microstructures under capillary forces — Part I: basic theory, *J. Microelectromech. Syst.*, 2 (1993) 33–43.
- [6] C.H. Mastrangelo and C.H. Hsu, Mechanical stability and adhesion of microstructures under capillary forces — Part II: experiments, *J. Microelectromech. Syst.*, 2 (1993) 44–55.
- [7] B. Bhushan (ed.), *Handbook of Micro/Nano Tribology*, CRC Press, New York, 1995.
- [8] J. Israelachvili, *Intermolecular and Surface Forces*, Academic Press, San Diego, 2nd edn., 1992.
- [9] K. Deng, R.J. Collins, M. Mehregany and C.N. Sukenik, Performance impact of monolayer coating of polysilicon micromotors, IEEE Micro Electro Mechanical Systems Workshop, Amsterdam, The Netherlands, 1995, pp. 368–373.
- [10] M.R. Houston, R. Maboudian and R.T. Howe, Ammonium fluoride anti-stiction treatments for polysilicon microstructures, Tech. Digest, 8th Int. Conf. Solid-State Sensors and Actuators (Transducers '95/Eurosensors IX), Stockholm, Sweden, 25–29 June, 1995, pp. 210–213.
- [11] M.R. Houston, R. Maboudian and R.T. Howe, Self-assembled monolayer films as durable anti-stiction coating for polysilicon microstructures, Solid-State Sensors and Actuators Workshop, Hilton Head Island, SC, USA, 1996, pp. 42–47.
- [12] R.L. Alley, P. Mai, K. Komvopoulos and R.T. Howe, Surface roughness modification of interfacial contacts in polysilicon microstructures, Proc. 7th Int. Conf. Solid-State Sensors and Actuators (Transducers '93), Yokohama, Japan, 7–10 June, 1993, pp. 288–291.
- [13] Y. Yee, K. Chun, J.D. Lee and C.-J. Kim, Polysilicon surface modification technique to reduce sticking of microstructures, *Sensors and Actuators A*, 52 (1996) 145–150.
- [14] H. Guckel, J.J. Sniegowski and T.R. Christenson, Advances in processing techniques for silicon micromechanical devices with smooth surfaces, IEEE Micro Electro Mechanical Systems Workshop, Salt Lake City, UT, USA, 1989, pp. 71–75.
- [15] N. Takashima, K.J. Gabriel, M. Ozaki, J. Takahashi, H. Horiguchi and H. Fujita, Electrostatic parallel-plate actuators, Proc. 6th Int. Conf. Solid-State Sensors and Actuators (Transducers '91), San Francisco, CA, USA, 24–28 June, 1991, pp. 63–66.
- [16] D. Kobayashi, T. Hirano, T. Furuhashi and H. Fujita, An integrated lateral tunneling unit, IEEE Micro Electro Mechanical Systems Workshop, Travemünde, Germany, 1992, pp. 214–219.
- [17] M. Orpana and A.O. Korhonen, Control of residual stress of polysilicon thin films by heavy doping in surface micromachining, Proc. 6th Int. Conf. Solid-State Sensors and Actuators (Transducers '91), San Francisco, CA, USA, 24–28 June, 1991, pp. 957–960.
- [18] G.T. Mulhern, D.S. Soane and R.T. Howe, Supercritical carbon dioxide drying of microstructures, Proc. 7th Int. Conf. Solid-State Sensors and Actuators (Transducers '93), Yokohama, Japan, 7–10 June, 1993, pp. 296–299.
- [19] C.H. Mastrangelo and G.S. Saloka, A dry-release method based on polymer columns for microstructure fabrication, Proc. IEEE Micro Electro Mechanical Systems, Fort Lauderdale, FL, USA, 1993, pp. 77–81.
- [20] D. Kobayashi, C.-J. Kim and H. Fujita, photoresist-assisted release of movable microstructures. *Jpn. J. Appl. Phys.*, 32 (1993) L1642–L1644.
- [21] Multi-User MEMS Processes (MUMPs) of the MCNC Center for Microelectronics Systems Technologies, Research Triangle Park, NC, USA.
- [22] T. Abe, W.C. Messner and M.L. Reed, Effective methods to prevent stiction during post-release-etch processing, IEEE Micro Electro Mechanical Systems Workshop, Amsterdam, The Netherlands, 1995, pp. 94–99.
- [23] G. Lin, C.-J. Kim, S. Konishi and H. Fujita, Design, fabrication, and testing of a C-shape actuator, Tech. Digest, 8th Int. Conf. Solid-State Sensors and Actuators (Transducers '95/Eurosensors IX), Stockholm, Sweden, 25–29 June, 1995, pp. 416–419.
- [24] J.H. Lee, K.H. Park, C.S. Lee, J.T. Baek, C.-J. Kim and H.J. Yoo, Fabrication of surface-micromachined polysilicon microactuators using HF gas-phase etching process, Proc. MEMS (DSC-Vol. 59), Int. Mechanical Engineering Congress and Exposition, Atlanta, GA, USA, Nov. 1996, pp. 373–377.
- [25] Y.-I. Lee, K.-H. Park, J. Lee, C.-S. Lee, H.J. Yoo, C.-J. Kim and Y.-S. Yoon, Dry release for surface micromachining with HF vapor-phase etching, *J. Microelectromech. Syst.*, 6 (1997) in press.

Biographies

Chang-Jin 'CJ' Kim received the Ph.D. degree in mechanical engineering from the University of California at Berkeley in 1991 with a study on MEMS (Topic: Polysilicon Microgrippers). He received the B.S. degree from Seoul National University and the M.S. degree from Iowa State University with the Graduate Research Excellence Award. He joined the faculty at UCLA in the Mechanical and Aerospace Engineering Department in 1993 after post-doctoral work at UC Berkeley and the University of Tokyo. His research is in MEMS, especially the issues related to mechanical engineering, including design and fabrication of microstructures, microactuators and systems, physics in microscale, and micromanufacturing. He has developed graduate courses in MEMS at UCLA and is also active in various MEMS professional courses. He is the recipient of the 1995 TRW Outstanding Young Teacher Award and the NSF CAREER Award. He served as chairman of the Micromechanical Systems Panel of the ASME Dynamic Systems and Control Division. He organized the Symposium on Micromechanical Systems and served as the chief editor of the *Proceedings of MEMS* for the 1996 ASME International Mechanical Engi-

neering Congress and Exposition. He also served as the Champion/Moderator for the 1996 ASME Satellite Broadcast Program, 'Microelectromechanical Systems (MEMS): Case Studies of Commercial Products'. Dr Kim is general co-chairman of the 6th IEEE International Conference on Emerging Technologies and Factory Automation (ETFA '97).

John Yehin Kim was born in 1971. He received his B.S. in mechanical engineering with emphasis on heat transfer and thermodynamics from the University of California, Los Angeles, in 1994. He is currently with the micro manufacturing laboratory at the University of California, Los Angeles, working on his master's degree in mechanical engineering with emphasis on micro electro mechanical systems. His research interests are in stiction reduction and various release

techniques in surface micromachining. He is also working for Allied Signal Aerospace in Torrance, California.

Balaji Sridharan was born in 1975. He received his B.Tech. degree in mechanical engineering from the Indian Institute of Technology, Madras, India in 1996. He is currently working towards his M.S. in manufacturing engineering at the University of California, Los Angeles, specializing in MEMS. He is working as a graduate student researcher with the Electrical Engineering Department at UCLA and was a teaching assistant in the Mechanical Engineering Department for the winter quarter of 1996. He is currently involved in research in the fields of MEMS packaging and stiction reduction methods. His research interests include micro-manufacturing, electronic and wafer-level packaging, as releasing methods for microelectromechanical systems.